

Determination of the s-phase formation coefficient of plasma nitrided austenitic steel

Bestimmung des s-Phasen-Bildungskoeffizienten plasmanitrierter austenitischer Stähle

P.M. Reinders¹, R.R. Patel¹, J. Musekamp², P. Kaestner¹, H. Hoche², G. Bräuer¹, M. Oechsner²

Plasma nitriding is an effective surface hardening treatment for austenitic stainless steels. During plasma nitriding, s-phase formation takes place which is not only responsible for high hardness and wear resistance but also for good corrosion resistance. In order to estimate the thickness of the s-phase for austenitic stainless steel in a plasma nitriding process, an empirical model is devised. A number of plasma nitriding processes of austenitic stainless steel (304 L) were carried out with varying treatment temperature from 360 °C to 450 °C and process duration ranging from 10 hours to 24 hours with constant pressure, voltage, pulse-to-pause-ratio and gas mixture. A time-temperature dependent s-phase formation coefficient is determined by measuring the thickness of the s-phase using a scanning electron microscope (SEM) and glow discharge optical emission spectroscopy (GDOES). The developed model is verified by three controlled experiments. This model fits the thickness of the s-phase with an error of less than 6 %.


Keywords: Plasma nitriding / s-phase / austenitic stainless steel / s-phase formation coefficient / model

Das Plasmanitrieren ist ein wirksames Verfahren zur Randschichthärtung von austenitischen Stählen. Während des Plasmanitrierens bildet sich die s-Phase, welche für eine hohe Härte, Verschleißfestigkeit und Korrosionsbeständigkeit verantwortlich ist. Um die Dicke der s-Phase eines austenitischen Stahls, welche sich während des Plasmanitrierens einstellt, im Vorfeld abschätzen zu können, wird ein empirisches Modell aufgestellt. Dazu werden verschiedene Plasmanitrierprozesse durchgeführt, die in der Behandlungstemperatur von 360 °C bis 450 °C und in der Behandlungsdauer von 10 Stunden bis 24 Stunden variiert werden. Andere Prozessparameter wie Druck, Spannung, Puls-Pause-Verhältnis oder Gaszusammensetzung bleiben konstant. Als Untersuchungswerkstoff dient der austenitische Stahl 1.4307. Ein abhängiger s-Phasen-Bildungskoeffizient wird durch das Mes-

¹ TU Braunschweig, Institut für Oberflächentechnik, Bienroder Weg 54 E, 24108, BRAUNSCHWEIG, FEDERAL REPUBLIC OF GERMANY

² TU Darmstadt, Zentrum für Konstruktionswerkstoffe MPA-IW, Grafenstraße 2, 64283, DARMSTADT, FEDERAL REPUBLIC OF GERMANY

Corresponding author: P.M. Reinders, TU Braunschweig, Institut für Oberflächentechnik, Bienroder Weg 54 E, 24108, BRAUNSCHWEIG, FEDERAL REPUBLIC OF GERMANY, E-Mail: p.reinders@tu-braunschweig.de

 This is an open access article under the terms of the Creative Commons Attribution Non-Commercial NoDerivs License, which permits use and distribution in any medium, provided the original work is properly cited, the use is non-commercial and no modifications or adaptations are made.

sen der s-Phasendicken unter Verwendung eines Rasterelektronenmikroskops (REM) und die Glimmentladungsspektroskopie (GDOES) bestimmt. Das entwickelte Modell wird durch Kontrollversuche unter selben obengenannten Bedingungen überprüft. Das Modell erlaubt die Abschätzung der s-Phasendicke mit einem Fehler von 6 %.

Schlüsselwörter: Plasmanitrieren / s-Phase / austenitischer Stahl / Bildungskoeffizient / Modell

1 Introduction

Austenitic stainless steels (ASSs) are widely employed in many industrial fields such as offshore installations, construction industry, medicine or chemical tanks due to their excellent corrosion resistance [1–3]. Unfortunately, they possess low hardness and therefore low wear resistance, which limits their service life in industrial applications [1, 4, 5]. By manipulating the superficial microstructure of austenitic stainless steel, the tribological properties can be enhanced. There are several methods through which an improvement of the surface properties of austenitic stainless steels can be achieved. Dissolution of interstitial elements such as carbon and nitrogen in the austenitic stainless steel matrix has a positive influence on the tribological properties [6].

Plasma nitriding is one of the techniques used to diffuse nitrogen superficially in the austenitic stainless steel matrix. Treatment temperatures should be below 450 °C to minimize the precipitation of chromium nitrides thereby retaining the corrosion resistance [6, 7–9]. In this manner, the superficial austenitic stainless steel layer is modified into s-phase which is a metastable phase supersaturated with nitrogen [3]. This modification brings along an improvement of hardness [4, 8, 10]. In the literature, there are divergent views about the influence of plasma nitriding on corrosion resistance and the implemented process parameters [4, 6, 10, 11].

The diffusion kinetics of nitrogen within the austenitic stainless steel matrix still remains to be fully understood, because many factors such as lattice structure, grain size, chemical composition, defect density and so on influence the diffusion process [9, 11]. All of this limits the industrial application of plasma nitriding treatment on a broader scale, as such data is necessary to tailor and optimize case hardening for specific industrial and commercial needs.

The present work focuses on the experimental study of the s-phase formed on AISI 304 L after plasma nitriding by varying the treatment temperature from 360 °C up to 450 °C for various process durations (from 10 h to 24 h). All other plasma nitriding parameters such as pressure, gas mixture or pulse-to-pause ratio remain unchanged. Time and temperature dependent s-phase formation coefficient was determined and a model was developed. With this model, the thickness of the s-phase for future plasma nitriding processes within the treatment temperature and process duration window can be estimated.

2 Material and methods

As examination material the austenitic stainless steel AISI 304 L was used, *Table 1*. A series of experiments on AISI 304 L austenitic stainless steel at temperatures in a range from 360 °C to 450 °C using pulsed-DC plasma nitriding with varying proc-

Table 1. Chemical composition of AISI 304 L austenitic stainless steel in weight percentage.

Tabelle 1. Chemische Zusammensetzung des austenitischen Stahls 1.4307 in Gewichtsprozent.

C	Si	Mn	P	S	Cr	Ni	N	Fe
0.030	1.00	2.00	0.045	0.030	17.5 – 19.5	8.0 – 10.5	0.10	Balance

ess duration was carried out, *Table 2*. The austenitic stainless steel was received in a plate and annealed form with a thickness of 5 mm which was then cut in square shape of dimension 20 mm × 20 mm. The surface was ground using silicon carbide grinding paper and polished to a mirror finish with a water-based monocrystalline diamond (3 μm) suspension to remove the passive film thereby improving the nitrogen diffusivity through the austenitic stainless steel matrix [3]. This also helps in obtaining a relatively even and smooth surface to avoid massive fluctuations in the thickness measurement of the s-phase. Sputter cleaning was conducted in an argon-hydrogen atmosphere before plasma nitriding with a pulsed-DC glow discharge, *Table 2*. In each plasma nitriding treatment, the specimens are surrounded by dummies on its perimeter to shield them from any arcing and avoid edge effect thereby circumventing any anomaly.

Shorter processes at the lowest treatment temperature of 360 °C were avoided, as diffusion is too low for such a short duration. For longer processes, however, the temperature was limited to the lower spectrum of the range to minimize the formation of chromium nitrides. Microstructure analyses of the cross-sectional micrographs were carried out on an optical and scanning electron microscope as well as glow discharge optical emission spectroscopy (Type „GDA 750“ from the company „Spectrums Analytik GmbH“). These cross-sections were

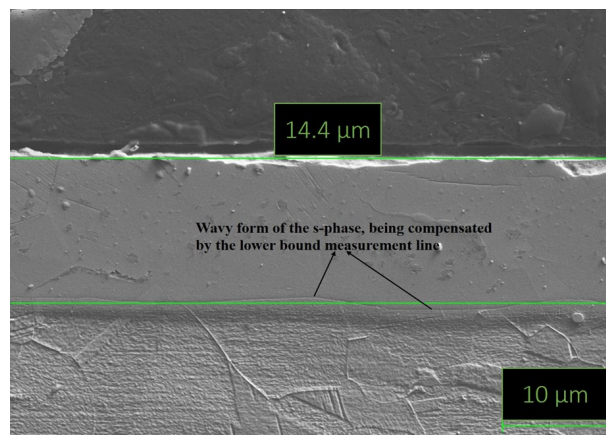


Figure 1. Exemplary measurement of the s-phase via scanning electron microscope.

Bild 1. Exemplarische Messung der s-Phase im Raster-elektronenmikroskop.

ground, polished and etched with a molybdenum etchant to reveal the nitrided layer. At high magnification (2000x), the cross-section of specimens is measured for the thickness of the s-phase via a scanning electron microscope, *Figure 1*. A total of five thickness measurements are taken per specimen.

Table 2. Nitriding parameters.

Tabelle 2. Nitrierparameter.

Process Steps	Temperature (°C)	Time (hours)	Pressure (Pa)	Voltage (V)	Pulse-pause ratio (μs)
Chamber evacuation	100	0.5	< 10	–	–
Sputtering & pre-heating	Depending on the plasma diffusion process	Till the desired temperature is achieved	130	400–500	100:1000 till 100:600
Plasma diffusion	390, 420 & 450	10	300	500	100:300
	390, 420 & 450	12			
	360, 390, 420 & 450	16			
	360, 390 & 420	20			
	360, 390 & 420	24			

Table 3. Measured s-phase thickness.**Tabelle 3.** Gemessene s-Phasendicke.

Process temperature	s-phase thickness with standard deviation (μm)				
	10 hours	12 hours	16 hours	20 hours	24 hours
360 °C	–	–	2.2 ± 0.1	2.3 ± 0.1	3.1 ± 0.1
390 °C	3.4 ± 0.1	3.8 ± 0.2	4.2 ± 0.3	4.3 ± 0.1	4.7 ± 0.1
420 °C	6.0 ± 0.3	6.1 ± 0.1	7.8 ± 0.2	8.3 ± 0.2	9.3 ± 0.2
450 °C	10.6 ± 0.5	12.1 ± 0.2	14.2 ± 0.3	–	–

3 Calculation of the s-phase formation coefficient

As mentioned above, the diffusion kinetics of nitrogen into the matrix of austenitic steel is a very complex phenomena which remains to be fully understood. For this reason, this study does not deal with the calculation of nitrogen's diffusion coefficient in austenitic steels, but rather with s-phase formation coefficient dependent on time and temperature. The following assumption was made to describe the s-phase formation coefficient:

The s-phase formation coefficient is a simplified form of the diffusion coefficient because the effective nitriding depth of nitrogen is higher than the thickness of the s-phase. This is because a certain concentration of nitrogen is necessary to distort the lattice structure of the austenitic steel matrix [11]. With this simple assumption, simplified diffusion laws can be used to describe the s-phase formation coefficient.

The growth kinetics of the s-phase depends directly on the nitrogen diffusion into the austenitic stainless steel matrix. This growth kinetics as a function of time can be represented by an equation, Equation 1. Where “x” is the mean distance by which the nitrogen molecules have traveled perpendicularly through the specimen surface in time “t” and “D” is the respective s-phase diffusion coefficient. This type of growth is called parabolic growth and the s-phase follows this law [7]. The simplified diffusion of nitrogen can be determined by empirical experiments and the thickness of the s-phase can be calculated under a given process duration, Equation 1.

$$\langle x^2 \rangle = 2 D t \quad (1)$$

4 Results

4.1 Thickness measurement of the s-phase

For the investigation 68 specimens were examined, which were subjected to a combination of process duration and treatment temperature resulting in 340 unique s-phase thicknesses, *Table 3*. The analysis of the results shows a clear dependence of the nitrogen-rich s-phase thickness on process duration and treatment temperature. The thicker the s-phase is, the more uneven the surfaces are. Whereas for thinner s-phase the surfaces are almost parallel and distortion-free. The s-phase thickness has been rounded to one decimal place accuracy. A systematic relationship of process duration and treatment temperature on the measured average s-phase thickness was found, *Table 3*. For better visualization of the tabulated data, some of the cross-sectional micrographs have been organized with the respect to process duration and treatment temperature, *Figures 2, 3*.

4.2 The growth kinetics of the s-phase

A positive influence of plasma nitriding duration and treatment temperature on the s-phase thickness can be deduced. The nitrogen concentration and the thickness of the s-phase depend on the nitriding depth, *Figure 4*. The measured thickness of the s-phase using glow discharge optical emission spectroscopy corresponds to that of measured via scanning electron microscope. Although it has to be noted that there is a threshold of minimum nitrogen

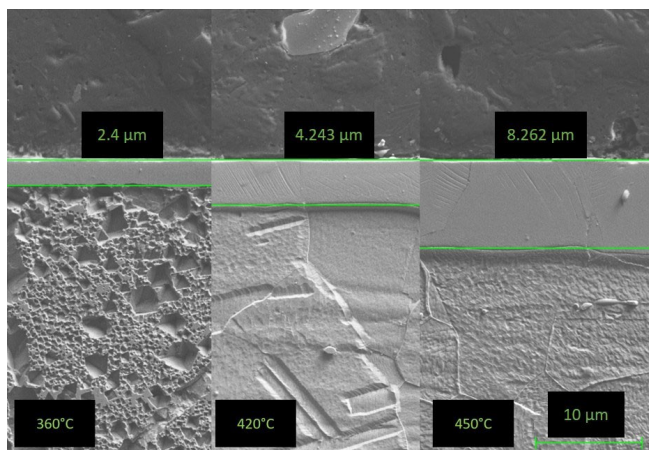


Figure 2. Influence of the plasma nitriding temperature on the thickness of the s-phase at a 20 hours treatment.

Bild 2. Einfluss der Temperatur des Plasmanitrierens auf die Dicke der s-Phase bei einer 20 stündigen Behandlung.

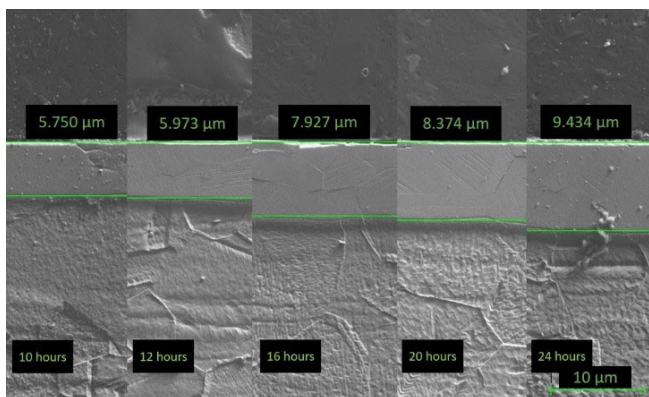


Figure 3. Influence of the plasma nitriding duration on the thickness of the s-phase at a 420 °C treatment.

Bild 3. Einfluss der Prozessdauer des Plasmanitrierens auf die Dicke der s-Phase bei einer Temperatur von 420 °C.

content in the s-phase. Beyond this threshold, it cannot be distinguished in a scanning electron microscope micrograph. Hence the glow discharge optical emission spectroscopy profiles are more pronounced compared to the scanning electron microscope micrographs. It can be concluded that the

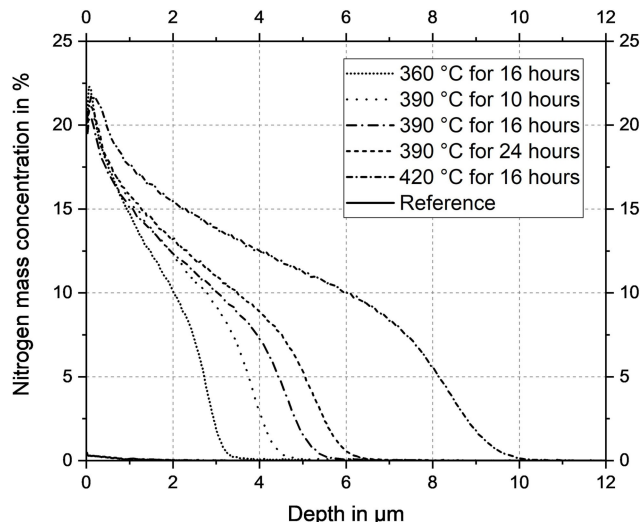


Figure 4. The nitrogen depth profile in mass percent for 5 different plasma nitrided samples (temperature/time) and the reference (1.4307).

Bild 4. Das Stickstofftiefenprofil in Massenprozent für 5 verschiedene plasmanitrierte Proben (Temperatur/Zeit) und die Referenz (1.4307).

higher the temperature and the longer the process duration, the deeper is the nitrogen penetration in the austenitic stainless steel matrix with respect to the observations via scanning electron microscope and glow discharge optical emission spectroscopy.

To find a pattern between the s-phase thickness and the variable factors, i.e. temperature and time, the data were visualized. In the present investigation, there are four process temperatures starting from 360 °C to 450 °C in 30 °C incremental steps. A regression line was generated for processes of the same temperature. If the gradient of the regression line is considered, it is noticeable that it increases with a certain factor, *Figure 5*. The values for the gradient of each regression line were calculated, *Table 4*.

Table 4. Experimentally determined degree gradient of the respective temperature.

Tabelle 4. Experimentell ermittelte Geradensteigung der jeweiligen Temperatur.

Temperature (T)	$T_0 = 360\text{ °C}$	$T_1 = 390\text{ °C}$	$T_2 = 420\text{ °C}$	$T_3 = 450\text{ °C}$
gradient (m)	$m_0 = 0.57127$	$m_1 = 1.01214$	$m_2 = 1.87847$	$m_3 = 3.48187$

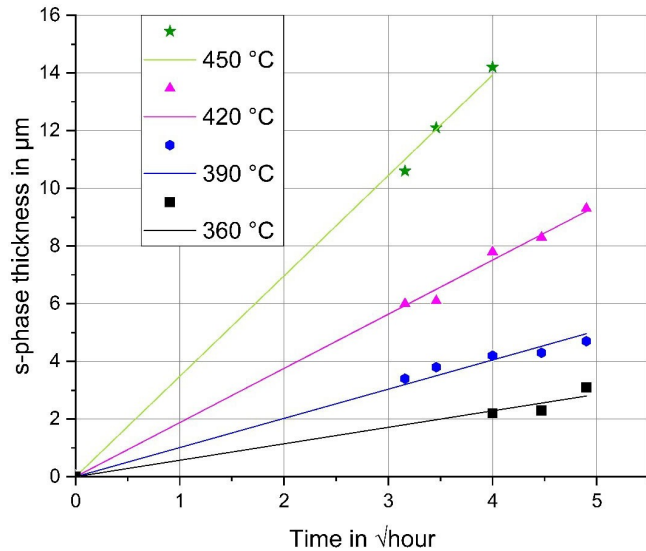


Figure 5. Time and temperature dependence of the s-phase thickness after the plasma nitriding treatment.

Bild 5. Zeit- und Temperatureinfluss auf die Dicke der s-Phase nach dem Plasmanitrieren.

4.3 Process modelling

The ratio of the gradient for the temperatures 390 °C and 360 °C gives a value of 1.77 (m_1/m_0). Implementing the same treatment for the remaining gradients yield two more values i.e. 1.855939 (m_2/m_1) and 1.853567 (m_3/m_2). Apart from the first ratio, the trend seems to give a constant ratio for two consecutive gradients, provided ΔT is constant. Considering this, the average of the above calculated three values is taken as the factor by which the gradient value grows for an increase in treatment temperature of 30 °C i.e. ΔT . The average value is calculated to be 1.82. Furthermore, to interpolate the gradient traced by any treatment temperature, T which lies between the temperature window, $T_n \geq T \geq T_0$, the arbitrary temperature is manipulated as an exponent whereas the factor by which the gradient increases is set as the base. Mathematically, the dependency of gradient to the treatment temperature can be generalized:

$$f(T, m) = m_0 \left\{ \sum_{i=1}^n \frac{1}{n} \left(\frac{m_i}{m_{i-1}} \right) \right\}^{\left(\frac{T-T_0}{\Delta T} \right)}$$

$$i \in N,$$

$$\Delta T = \left(\frac{T_n - T_0}{n} \right) \neq 0,$$

$$T_n \geq T \geq T_0$$

$$f(T, m) = m_0 \left\{ \sum_{i=1}^n \frac{1}{n} \left(\frac{m_i}{m_{i-1}} \right) \right\}^{n \left(\frac{T-T_0}{T_n-T_0} \right)}$$

The equation can be decomposed into two parts. Firstly, m_0 is the gradient traced by the lower bound treatment temperature (T_0) which remains a constant and secondly, the term following m_0 is always greater than unity for any temperature (T) greater than the lower bound treatment temperature (T_0). This is because the exponent part with the combination of the base (which in turn is an average ratio of consecutive gradients) is always greater than unity. For example, if the treatment temperature is taken as T_0 , the exponent part reduces to zero hence the whole term followed by m_0 becomes unity. Ultimately giving the final value m_0 , whereas for temperature more than T_0 the combination of base and exponent always yields a final value which is more than unity. Hence, for any temperature higher than the lower bound treatment temperature, the gradient value increases, Equation 3. As shown in the next section, the process can be modelled satisfactorily

4.4 Application of the model

The model offers a powerful tool to predict s-phase thickness for an arbitrary treatment temperature within the given process temperature window for a specific process duration. Let m_T be a gradient traced out by a process carried out at temperature “ T ” which lies within the selected treatment temperature window ($T_n > T > T_0$). The value of m_T can be interpolated, Equation 4.

$$m_T = m_0 \left\{ \sum_{i=1}^n \frac{1}{n} \left(\frac{m_i}{m_{i-1}} \right) \right\}^{n \left(\frac{T-T_0}{T_n-T_0} \right)} \quad (4)$$

$$m_0 \leq m_T \leq m_n$$

The model can be simplified by using the experimentally measured gradients, Equations 5–7.

$$m_T = m_0 \left\{ \frac{1}{3} \left(\frac{m_1}{m_0} + \frac{m_2}{m_1} + \frac{m_3}{m_2} \right) \right\}^{3 \left(\frac{T-T_0}{T_3-T_0} \right)} \quad (5)$$

$$m_T = 0.57127 \left\{ \frac{1}{3} \left(\frac{1.01214}{0.57127} + \frac{1.87847}{1.01214} + \frac{3.48187}{1.87847} \right) \right\}^{3 \left(\frac{T-360}{450-360} \right)} \quad (6)$$

$$m_T = 0.57127 \{6.09921\}^{\left(\frac{T-360}{90} \right)} \quad (7)$$

To be able to predict the s-phase thickness for different temperatures, the temperature-dependent gradients were interpolated, Figure 6. The model is derived by a nonlinear regression method in conjunction with the power-law. A total of ninety-one equispaced nodes are used for the same, starting from 360 °C to 450 °C. Each node represents the temperature in an integer form, although temperature can also exist in decimal form, in the present

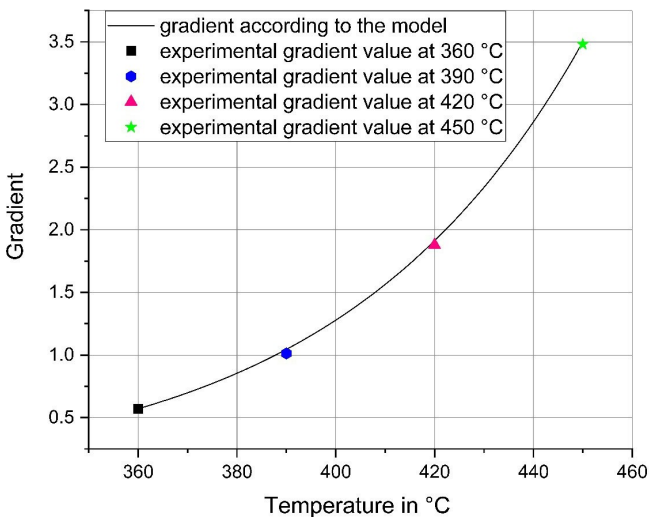


Figure 6. Influence of the plasma nitriding temperature on the gradient.

Bild 6. Einfluss der Plasmanitriertemperatur auf den Gradienten.

investigation only integers are considered. For this reason, the model curve looks smooth globally but locally it possesses a discrete form.

4.5 Controlled experiment and result verification

To check the validity of the developed model, three controlled experiments were conducted. All the plasma nitriding parameters were kept constant apart from the treatment temperature and process duration, Table 5. To verify whether the experimental results agree with the process model, the previously determined equation was used, Equation 7.

$$m_{375} = 0.57127 \{6.09921\}^{\left(\frac{375-360}{90} \right)}$$

$$m_{375} = 0.77218$$

Once the gradient value is calculated, the s-phase thickness can be deduced according to the parabolic growth law, Figure 6. In the below equation, “x” is the s-phase thickness in μm and “t” is the process duration in hour.

$$m_{375} = \frac{x_{375}}{\sqrt{t}}$$

$$x_{375} = 0.77218 \sqrt{18} \mu\text{m} \quad (8)$$

$$x_{375} = 3.27 \mu\text{m}$$

The same treatment is applied to the remaining two controlled experiments which gives the s-phase thickness of $x_{405} = 5.27 \mu\text{m}$ and $x_{435} = 8.15 \mu\text{m}$ respectively. With the s-phase thickness known for the given treatment temperature and process duration, the gradient traced by the three controlled experiments can be compared against the process

Table 5. Controlled experiment parameters.

Tabelle 5. Parameter der Kontrollversuche.

Experiment number	Treatment temperature (°C)	Process duration (hours)
1	375	18
2	405	14
3	435	10

model. The modelled gradient values match with the controlled experimental gradient values, *Figure 7*.

The experimental and the modelled s-phase thickness are compared and the relative error of the model is determined. The modelled and actual s-phase thickness does not show extreme disparity and a maximum relative error of only 5.48 % is recorded, *Table 6*. The disparity in the modelled and actual value arises from a variety of reasons. One of them is that the treatment temperature in any plasma nitriding treatment does not discretely jump

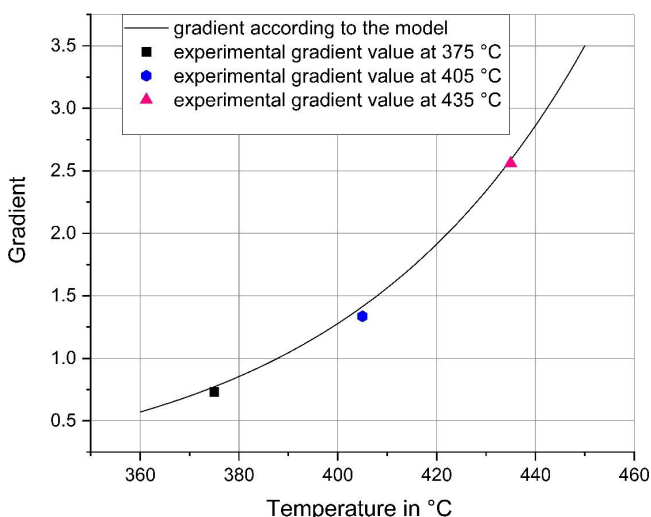


Figure 7. Comparison of the measured and modelled gradient after controlled experiments.

Bild 7. Vergleich des gemessenen und modellierten Gradienten nach Kontrollversuchen.

Table 6. S-phase thickness of the controlled experiments and relative error of modelled values against experimental ones.

Tabelle 6. S-Phasendicke der Kontrollversuche und der relative Fehler des Modells gegenüber der gemessenen s-Phasendicke.

Process parameter	s-phase thickness according to the model (μm)	Experimental s-phase thickness (μm)	Relative error
375 °C for 18 hours	3.27	3.1 ± 0.1	5.48 %
405 °C for 14 hours	5.27	5.0 ± 0.1	5.40 %
435 °C for 10 hours	8.15	8.1 ± 0.1	0.61 %

to the target temperature, rather it smoothly rises from the room temperature to the final treatment temperature. For thicker s-phase only a tiny relative error is present compared to the relatively thinner s-phases.

5 Conclusion

In this study, a model was developed which allows determining the thickness of the s-phase for a plasma nitriding process at a given treatment temperature and process duration for the austenitic steel 304 L. A number of treatment temperatures starting from 360 °C to 450 °C and process duration between 10 hours and 24 hours were considered. By measuring the s-phase thickness, a temperature-dependent gradient was determined.

Based on these gradients, a model curve was generated which allows the calculation of s-phase thickness recursively for other treatment temperatures and process duration in the chosen area. The controlled experiments showed that the model deviates from the actual measurements with a maximum relative error of 5.48 %. To further develop the model and apply it to other austenitic steels, a factor for the elemental composition is included in current investigations. Further process parameters that influence the thickness of the s-phase such as pressure, voltage, pulse-to-pause-ratio and gas mixture are to be incorporated by additional factors.

Acknowledgements

This research work was funded by the Deutsche Forschungsgemeinschaft (DFG) – Project „Wechselwirkung zwischen dem Ausgangs-Gefügezustand und den daraus folgenden Eigenschaften plasmnitrierter austenitischer Stähle“ (DFG-Geschäftszeichen HO 3315/19-1 und BR 2178/41-1). Open access funding enabled and organized by Projekt DEAL

6 References

- [1] Y. Zhao, B. Yu, L. Dong, Hao Du, J. Xiao, *Surface and Coatings Technology* **2012**, 210, 90.
- [2] Y. Hoshiyama, R. Mizobata, H. Miyake, *Surface and Coatings Technology* **2016**, 307, 1041.
- [3] M. Chemkhi, D. Restraint, A. Roos, C. Garnier, L. Waltz, C. Demangel, G. Proust, *Surface and Coatings Technology* **2013**, 221, 191.
- [4] F. Borgioli, E. Galvanetto, T. Bacci, *Vacuum* **2016**, 127, 51.
- [5] S.J. Ji, L. Wang, J.C. Sun, Z.K. Hei, *Surface and Coatings Technology* **2005**, 195, 81.
- [6] E. Menthe, A. Bulak, J. Olfe, A. Zimmermann, K.-T. Rie, *Surface and Coatings Technology* **2000**, 133, 259.
- [7] S. Mändl, R. Dunkel, D. Hirsch, D. Manova, *Surface and Coatings Technology* **2014**, 258, 722.
- [8] A. Martinavičius, G. Abrasonis, A.C. Scheinost, R. Danoix, F. Danoix, J.C. Stinville, G. Talut, C. Templier, O. Liedke, S. Gemming, W. Möller, *Acta Materialia*, **2012**, 60, 4065.
- [9] A. Martinavičius, *Dissertation*, Technische Universität Dresden, Dresden **2010**.
- [10] Q. Luo, O. Oluwafemi, M. Kitchen, S. Yang, *Wear* **2017**, 376, 1640.
- [11] J. Biehler, *Dissertation*, Technische Universität Darmstadt, Darmstadt **2016**.

Received in final form: June 8th 2020